

# Synthesis and Biological Evaluation of New Triazolo- and Imidazolopyridine ROR $\gamma$ t Inverse Agonists

Samuel Hintermann,<sup>[a]</sup> Christine Guntermann,<sup>[b]</sup> Henri Mattes,<sup>[a]</sup> David A. Carcache,<sup>[a]</sup> Juergen Wagner,<sup>[a]</sup> Anna Vulpetti,<sup>[a]</sup> Andreas Billich,<sup>[b]</sup> Janet Dawson,<sup>[b]</sup> Klemens Kaupmann,<sup>[b]</sup> Joerg Kallen,<sup>[c]</sup> Rowan Stringer,<sup>[d]</sup> and David Orain\*<sup>[a]</sup>

Retinoic-acid-related orphan receptor  $\gamma$ t (ROR $\gamma$ t) is a key transcription factor implicated in the production of pro-inflammatory Th17 cytokines, which drive a number of autoimmune diseases. Despite diverse chemical series having been reported, combining high potency with a good physicochemical profile has been a very challenging task in the ROR $\gamma$ t inhibitor field. Based on available chemical structures and incorporating in-house knowledge, a new series of triazolo- and imidazopyridine ROR $\gamma$ t inverse agonists was designed. In addition, replacement of the terminal cyclopentylamide metabolic soft spot by five-membered heterocycles was investigated. From our efforts, we identified an optimal 6,7,8-substituted imidazo[1,2-*a*]pyridine core system and a 5-*tert*-butyl-1,2,4-oxadiazole as cyclopentylamide replacement leading to compounds **10** ((*S*)-*N*-(8-((4-(cyclopentanecarbonyl)-3-methylpiperazin-1-yl)methyl)-7-methylimidazo[1,2-*a*]pyridin-6-yl)-2-methylpyrimidine-5-carboxamide) and **33** ((*S*)-*N*-(8-((5-(*tert*-butyl)-1,2,4-oxadiazol-3-yl)-3-methylpiperazin-1-yl)methyl)-7-methylimidazo[1,2-*a*]pyridin-6-yl)-2-methylpyrimidine-5-carboxamide). Both derivatives showed good pharmacological potencies in biochemical and cell-based assays combined with excellent physicochemical properties, including low to medium plasma protein binding across species. Finally, **10** and **33** were shown to be active in a rodent pharmacokinetic/pharmacodynamic (PK/PD) model after oral gavage at 15 mg kg<sup>-1</sup>, lowering IL-17 cytokine production in ex vivo antigen recall assays.

Two isoforms, RORCvar1 (also known as ROR $\gamma$ 1) and the T-cell-specific RORCvar2 (ROR $\gamma$ 2, ROR $\gamma$ t) have been identified. RORCvar2 is considered an attractive drug target based on its involvement in the production of pro-inflammatory Th17 cytokines, such as IL-17, which drive a number of autoimmune diseases.<sup>[1–3]</sup> Owing to the structural identity of the ligand-binding domains of the two RORC isoforms, it is highly unlikely that RORCvar2-specific inhibitors will be identified which do not also inhibit RORCvar1. A plethora of structurally diverse RORC inhibitors<sup>[4]</sup> have been described blocking Th17 differentiation in vitro, and selected examples have also been reported to inhibit inflammation in rodent in vivo models of autoimmune disease.<sup>[2]</sup> Successful clinical outcomes with several anti-IL-17 antibodies have validated the IL-17 pathway as a key pathway for the treatment of inflammation. Recently, Vitae Pharmaceuticals reported a first successful four-week clinical proof-of-concept trial with the RORC inhibitor VTP-43742<sup>[5]</sup> for the treatment of psoriasis.

In recent years, the vast majority of reported ROR $\gamma$ t inverse agonists use the alkyl aryl sulfone warhead first described by GlaxoSmithKline (GSK) researchers,<sup>[6]</sup> including the likely clinical candidate from Vitae Pharmaceuticals (**1**, Figure 1). Compound **1** contains an interesting weakly basic center that may confer some advantageous physicochemical properties. Indeed, combining high potency and good solubility has been a very challenging task in the RORC inhibitor field. Along the same lines, in 2014 GSK scientists reported a new class of compounds

Retinoic-acid-related orphan receptor C (RORC) is a nuclear hormone receptor that plays an important role in immunity.

[a] Dr. S. Hintermann, Dr. H. Mattes, Dr. D. A. Carcache, Dr. J. Wagner, Dr. A. Vulpetti, Dr. D. Orain  
Global Discovery Chemistry, Novartis Institutes for BioMedical Research, Novartis Campus, 4002 Basel (Switzerland)  
E-mail: david.orain@novartis.com

[b] Dr. C. Guntermann, Dr. A. Billich, Dr. J. Dawson, Dr. K. Kaupmann  
ATI, Novartis Institutes for BioMedical Research, Novartis Campus, 4002 Basel (Switzerland)

[c] Dr. J. Kallen  
CPC, Novartis Institutes for BioMedical Research, Novartis Campus, 4002 Basel (Switzerland)

[d] Dr. R. Stringer  
MAP, Novartis Institutes for BioMedical Research, Novartis Campus, 4002 Basel (Switzerland)

Supporting information and the ORCID identification number(s) for the author(s) of this article can be found under <http://dx.doi.org/10.1002/cmdc.201600500>.

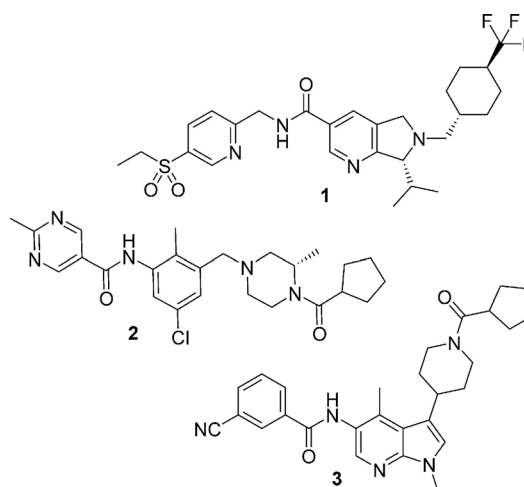


**Figure 1.** Selected examples of ROR $\gamma$ t inverse agonists from the patent literature: Putative clinical candidates from Vitae Pharmaceuticals (**1**),<sup>[5]</sup> GSK (**2**), and Pfizer (**3**).

(e.g., **2**, Figure 1) containing a weakly basic center and claiming *in vivo* activity after oral dosing.<sup>[7]</sup> A few months later, a new patent application from Pfizer disclosed a very similar series of compounds (e.g., **3**, Figure 1), but which lack the basic center.<sup>[8]</sup> Herein we present our efforts toward triazolo- and imidazopyridine central core analogues of compound **2** as novel ROR $\gamma$ t inhibitors with some improved properties.

The first imidazopyridine system was constructed from commercially or synthetically available precursor **4** bearing a nitro group on its western face as precursor for the amide nitrogen, and a bromo group on its eastern face allowing introduction of the benzylpiperazine motif. Direct cyclization with chloroacetaldehyde led to formation of the corresponding imidazopyridine **5** in good yield. After nitro group reduction and coupling with 2-methylpyrimidine-5-carboxylic acid, the corresponding amide **7** was obtained. Introduction of the key benzyl piperazine motif was realized via a Suzuki-type coupling using the preformed trifluoroborate methylpiperazine salt **8**.<sup>[9]</sup> After Boc group deprotection and amide formation, the first final derivative **10** was obtained. Aromatic amide cleavage under basic conditions led to the versatile aniline intermediate **11**, allowing exploration of the western part. As an illustrative example, synthesis of the corresponding methylpyridine amide **12** is described (Scheme 1).

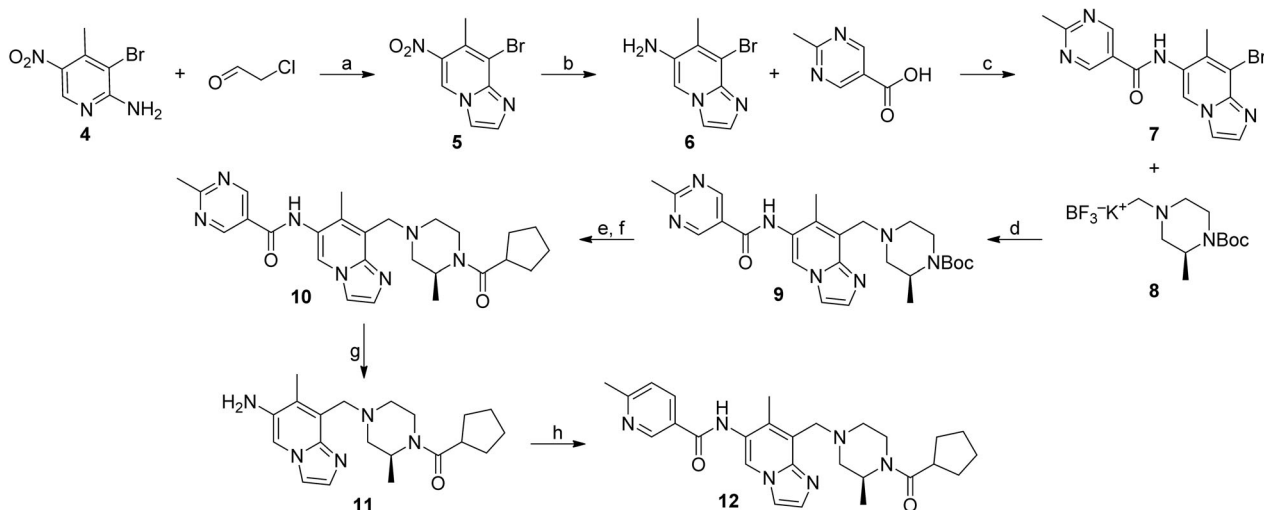
A second imidazopyridine ring system was synthesized using a completely different approach for introduction of the western and eastern substituents. Starting from commercial derivative **13**, the corresponding *N*-oxide **14** was rearranged to the 2-*tert*-butylamino intermediate, yielding the aminopyridine **15** after *tert*-butyl group removal.<sup>[10]</sup> The imidazopyridine ring system was constructed as before by cyclization with chloroacetaldehyde under basic conditions. The aniline as precursor for the nitrogen amide on the western face was introduced via

Buchwald coupling of **17** with dimethoxybenzylamine and subsequent acid-catalyzed deprotection to afford intermediate **18**. For the eastern face, the ester group was reduced to the corresponding alcohol after reduction with lithium aluminum hydride and then converted into the benzylic chloride intermediate **19** with thionyl chloride. Nucleophilic substitution of **19** with the preformed piperazine amide **20**<sup>[7a]</sup> led to aniline **21**, which was finally acetylated to afford final derivative **22** in moderate yield (Scheme 2).

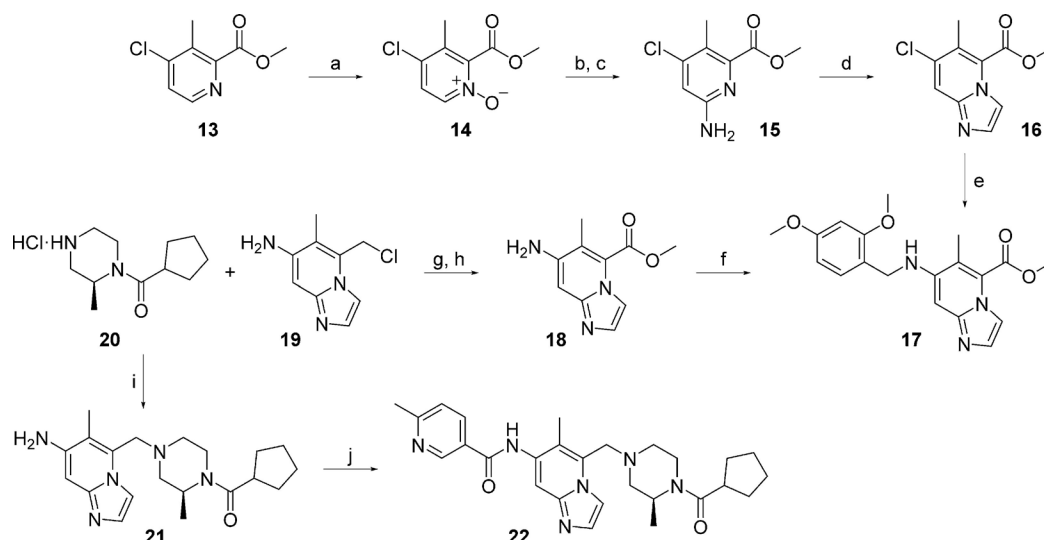
Next, synthesis of the triazolopyridine ring system was carried out by starting from commercially available precursor **23**, which was reacted with hydrazine hydrate to yield intermediate **24**. Cyclization with trimethyl orthoformate or trimethyl orthoacetate gave access to the corresponding triazolopyridine intermediates in very high yield, bearing at C2 an H atom for **25** or a methyl substituent for **25a**. Following a similar sequence as described in Scheme 1, final derivatives **29** and **30** were synthesized. Notably, nitro group reduction proved to be much more challenging for **25** than for **25a**. Only reduction with iron in acetic acid at room temperature for a short period of time led to the desired aniline **26** in an acceptable yield (Scheme 3).

Intermediates **31** or **32** were synthesized according to procedures described in Scheme 1, and all *N*-oxadiazole *tert*-butyl isomers were prepared analogously to well-described published procedures,<sup>[11]</sup> leading to final derivatives **34–36**. Synthesis of isoxazole derivative **37** was achieved by cyclization of the intermediate thioamide with hydroxylamine. Finally, *N*-pyrimidine analogue **38** was obtained in moderate yield by nucleophilic aromatic substitution (Scheme 4).

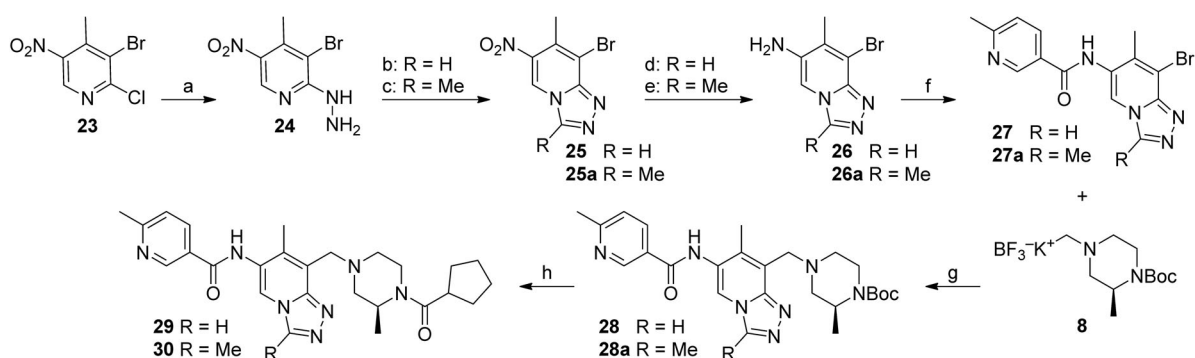
Our *in vitro* screening cascade started with a biochemical fluorescence resonance energy transfer (FRET) assay that measures inhibition of RIP140 co-activator peptide binding to the



**Scheme 1.** Synthesis of imidazopyridine derivatives **10** and **12**. *Reagents and conditions:* a) chloroacetaldehyde 50 wt% in H<sub>2</sub>O (4 equiv), 90 °C, 3 h (crude); b) Fe (2 equiv), NH<sub>4</sub>Cl (5.3 equiv), EtOH, reflux, 18 h (crude); c) acid (1.25 equiv), TEA (3 equiv), propylphosphonic anhydride (T3P) 50 wt% in EtOAc (1.5 equiv), CH<sub>2</sub>Cl<sub>2</sub>, RT, 18 h (42% yield over three steps); d) compound **8** (1.2 equiv), Pd(OAc)<sub>2</sub> (0.05 equiv), X-Phos (0.1 equiv), Cs<sub>2</sub>CO<sub>3</sub> (2.5 equiv), THF/H<sub>2</sub>O (10:1), 90 °C, 40 h (79% yield); e) 4 M HCl in dioxane, CH<sub>2</sub>Cl<sub>2</sub>, RT, 2 h (quant.); f) cyclopentanecarboxylic acid (1 equiv), DIPEA (5 equiv), T3P 50 wt% in EtOAc (1.2 equiv), CH<sub>2</sub>Cl<sub>2</sub>, RT, 18 h (72% yield); g) NaOH 1 M (3 equiv), MeOH, 120 °C, 6 h; h) 6-methylnicotinic acid (1.1 equiv), T3P 50% in EtOAc (1.3 equiv), TEA (3 equiv), CH<sub>2</sub>Cl<sub>2</sub>, RT, 48 h (28% yield over two steps).



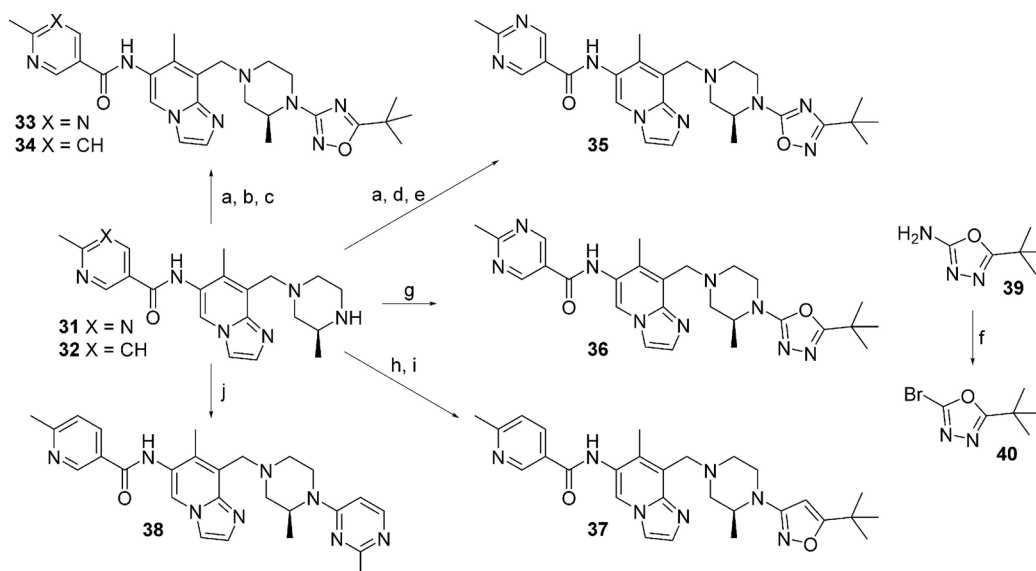
**Scheme 2.** Synthesis of imidazopyridine derivative **22**. *Reagents and conditions:* a) *m*CPBA (1.2 equiv),  $\text{CH}_2\text{Cl}_2$ , RT, 48 h (83% yield); b) *t*BuNH<sub>2</sub> (7 equiv),  $\text{Ts}_2\text{O}$  (3.3 equiv),  $\text{CH}_2\text{Cl}_2/\text{PhCF}_3$  (4/1), 0 °C, 1 h (68% yield); c) TFA,  $\text{CH}_2\text{Cl}_2$ , 70 °C, 12 h (74% yield); d) chloroacetaldehyde 50 wt % in  $\text{H}_2\text{O}$  (5 equiv), NaHCO<sub>3</sub> (2 equiv), MeOH, 70 °C, 24 h (70% yield); e) 2,4-dimethoxybenzylamine (1.5 equiv), BrettPhos precat (0.2 equiv), Cs<sub>2</sub>CO<sub>3</sub> (3 equiv), dioxane, 70 °C, 2 h (45% yield); f) 4 M HCl dioxane, RT, 1 h (98% yield); g) LiAlH<sub>4</sub> 2 M in THF (1 equiv), THF, 0 °C, 10 min (69% yield); h) SOCl<sub>2</sub> (10 equiv), dioxane, RT, 12 h (59% yield); i) **20** (1.1 equiv), DIPEA (3.5 equiv), CH<sub>3</sub>CN, 70 °C, 16 h (99% yield, 78% purity); j) 6-methylnicotinoyl chloride (1.1 equiv), DIPEA (4 equiv),  $\text{CH}_2\text{Cl}_2$ , RT, 12 h (8% yield).



**Scheme 3.** Synthesis of triazolopyridines **29** and **30**. *Reagents and conditions:* a) hydrazine hydrate (30 equiv), dioxane, 10 °C, 15 h (90% yield); b) trimethyl orthoformate (10 equiv), reflux, 1 h (97% yield); c) trimethyl orthoacetate (9 equiv), reflux, 2 h (90% yield); d) Fe (5 equiv), AcOH, RT, 3 h (50% yield); e) Fe (2 equiv), NH<sub>4</sub>Cl (5 equiv), MeOH, reflux, 18 h (42% yield, 75% purity); f) 6-methylnicotinoyl chloride (1.3 equiv), pyridine (3 equiv),  $\text{CH}_2\text{Cl}_2$ , RT, 12 h (44% yield for **27** and 64% yield for **27a**); g) compound **8** (1.2 equiv), Pd(OAc)<sub>2</sub> (0.05 equiv), X-Phos (0.1 equiv), Cs<sub>2</sub>CO<sub>3</sub> (2.5 equiv), THF/ $\text{H}_2\text{O}$  (10:1), 90 °C, 18 h (23% yield for **28** and 69% yield for **28a**); h) 1. 4 M HCl in dioxane,  $\text{CH}_2\text{Cl}_2$ , RT, 16 h (quant.), then 2. cyclopentanecarbonyl chloride (1 equiv), DIPEA (5 equiv),  $\text{CH}_2\text{Cl}_2$ , 0 °C, 30 min (11% yield for **29** and 80% yield for **30**).

human ROR $\gamma$ t ligand binding domain (LBD). To demonstrate cellular potency against ROR $\gamma$ t, a Gal4 reporter gene assay was established using Jurkat cells stably expressing constructs consisting of the Gal4 DNA binding domain fused to the ROR $\gamma$ -hinge-LBD and Gal4 upstream activator sequences driving transcription of the luciferase firefly gene. Next, the compounds were assessed for their ability to inhibit IL-17A production by primary human CD4 T cells under conditions that favor Th17 differentiation. To determine whether ROR $\gamma$ t inverse agonists are potent in the presence of blood cells and plasma proteins, 20% human whole blood was stimulated with lectin concanavalin A (ConA) and IL-23, and inhibition of IL-17A secretion was measured by enzyme-linked immunosorbent assay (ELISA), the results of which are listed in Table 1.

Compound **2** proved to be a very potent ROR $\gamma$ t inverse agonist across all assays tested. From its physicochemical profile, **2** showed moderate solubility at neutral pH and relatively low stability in human liver microsomes (HLM), whereas the compound was more stable when incubated with rat liver microsomes (RLM). In vitro and in vivo metabolism studies identified the cyclopentyl ring as the main weak spot that was prone to oxidation. First, however, we turned our attention to modifications of the central phenyl core in order to improve the physicochemical properties of the scaffold. Based on modeling, [6,5]-fused heterocyclic systems were assessed. We decided to keep as one exit vector the basic nitrogen atom of the piperazine motif in contrast to compound **3**. The first analogues designed were based on a 6,7,8-substituted imidazo[1,2-*a*]pyridine core, and derivatives **10** and **12** were synthesized. Com-



**Scheme 4.** Synthesis of *N*-heteroaryl piperazine imidazopyridines **35–38**. *Reagents and conditions:* a) BrCN, DIPEA, CH<sub>2</sub>Cl<sub>2</sub>, 0 °C, 1 h; b) H<sub>2</sub>NOH, EtOH, 90 °C, 2.5 h; c) (tBuCO)<sub>2</sub>O, pyridine, 120 °C, 3 h (overall yield 23% for **33** and 45% for **34**); d) tBuC(NH)NHOH, ZnCl<sub>2</sub>, EtOH, 4 days; e) 4 M HCl, EtOH, 80 °C, 24 h (13% overall yield); f) CuBr<sub>2</sub>, tBuONO, MeCN, RT, 2 h (81% yield); g) compound **40**, K<sub>2</sub>CO<sub>3</sub>, DMF, 90 °C, 16 h (31% yield); h) tBuCOCH<sub>2</sub>C(=S)Me, TEA, EtOH, 100 °C, 20 h (25% yield); i) H<sub>2</sub>NOH, EtOH, reflux, 28 h (26% yield); j) 4-bromo-2-methylpyrimidine, DIPEA, butanol, 120 °C, 11 h (9% yield).

**Table 1.** In vitro pharmacological and physicochemical profile of compounds **2**, **10**, **12**, **22**, **29**, **30**, and **33–38**.

Compd	FRET <sup>[c]</sup>	IC <sub>50</sub> [nM] (inhib. [%]) <sup>[a,b]</sup>		hu-WB <sup>[f]</sup>	HT-Sol. [mg L <sup>-1</sup> ] <sup>[g]</sup>	cLogP	MDCK P <sub>app</sub> A→B [10 <sup>-6</sup> cm s <sup>-1</sup> ]	LM CL <sub>int</sub> [μL (min mg) <sup>-1</sup> ]	
		Gal4 <sup>[d]</sup>	hu-Th17 <sup>[e]</sup>					Rat	Human
<b>2</b>	1 (99)	32 (97)	13 (81)	35 (89)	57	3.5	11.7	33	97
<b>10</b>	13 (97)	324 (97)	171 (78)	168 (83)	127	2.0	15.7	30	30
<b>12</b>	10 (98)	194 (97)	73 (80)	171 (83)	443	2.9	16.4	75	58
<b>22</b>	3 (94)	162 (96)	177 (79)	207 (82)	48	2.9	12.1	453	168
<b>29</b>	15 (94)	2147 (95)	NT	NT	367	1.9	NT	<25	<25
<b>30</b>	37 (95)	7271 (86)	NT	NT	12	2.2	16.6	148	36
<b>33</b>	2.3 (99)	164 (97)	124 (78)	282 (82)	343	2.6	18.3	<25	96
<b>34</b>	3 (97)	100 (97)	71 (79)	161 (83)	119	3.6	4.5	41	171
<b>35</b>	10 (98)	303 (97)	NT	NT	276	2.6	19	<25	69
<b>36</b>	23 (96)	1166 (97)	NT	NT	>504	1.8	4.7	<25	<25
<b>37</b>	1 (98)	110 (97)	101 (82)	331 (86)	148	4.0	9.4	49	94
<b>38</b>	893 (87)	NT	NT	NT	>471	2.7	5.5	<25	61

[a] Values are the mean of at least three independent measurements. [b] In parentheses: maximum inhibition at 10 μM. [c–f] See the Experimental Section for assay descriptions. [g] Solubility at pH 6.8. NT: Not tested.

compound **10**, with the 4-methylpyrimidine amide, showed relatively weak potency in the FRET and Gal4 assays, with IC<sub>50</sub> values of 13 and 324 nM, respectively. Surprisingly, almost identical potencies, around 170 nM, were observed in the human Th17 assays with or without the addition of blood. Introduction of this imidazo[1,2-*a*]pyridine central core decreases the lipophilicity by 1.5 log units relative to **2** and consequently the solubility was improved while keeping the high permeation as measured in the MDCK permeability assay. In addition, the new core nicely increases the stability in the liver microsome assays, particularly for the HLM assay. The analogous 4-methylpyridine amide **12** showed a similar profile to that of **10**, but was less stable when incubated with RLM and HLM.

Next, a second regioisomer of the 5,6,7-substituted imidazo[1,2-*a*]pyridine system was studied. The analogous 4-methylpyridine amide **22** was synthesized as described and compared

with **12**. Despite being more potent in the biochemical read-out, **22** showed the same pharmacological profile as **12** in the cellular assays. This regioisomer also showed lower solubility and much higher instability toward RLM and HLM. Therefore, we decided to keep the nitrogen architecture of the first imidazopyridine isomer constant. By adding another nitrogen atom, a corresponding triazolopyridine system was synthesized with either hydrogen **29** or a methyl substituent **30** attached to the triazole ring. Despite being nearly equipotent in the biochemical assay, in the 10 nM range, **29** was almost 10 times less potent in the Gal4 cellular assay than the imidazopyridine analogue **12**. The reason for this discrepancy is not understood, as no clear change in permeation properties were observed. Whilst this core change had a negative impact on cell potency, it was rather beneficial for microsomal stability, with clearance in both RLM and HLM below the level of detection.

The methyl triazole analogue **30** showed decreased potency in the biochemical and Gal4 assays pointing toward steric interference with the binding pocket. In summary, the first round of optimization led to the discovery of a new heterocyclic central core with improved solubility and human microsomal stability whilst keeping good on-target potency.

An X-ray structure of **10** bound to ROR $\gamma$ t was obtained at 1.77 Å resolution using the ROR $\gamma$ t (264–491) construct, that is, with the C-terminal helix 12 deleted (Figure 2). The two nitro-

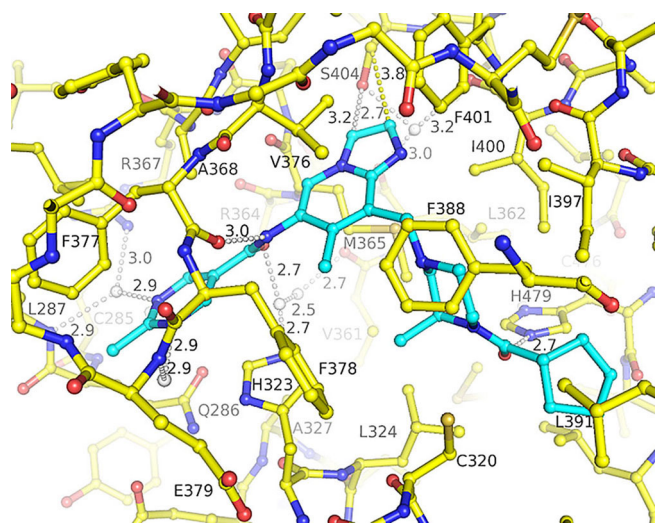


**Figure 2.** X-ray structure (1.77 Å resolution) of the ligand binding domain of ROR $\gamma$ t (carbon atoms in yellow, nitrogen atoms in blue, oxygen atoms in red, and sulfur atoms in brown) bound to compound **10** (carbon atoms in cyan), zoomed in at the ligand binding pocket. Selected water molecules and hydrogen bond interactions are shown in white, and a selected van der Waals interaction in yellow. Details of this X-ray structure determination will be published elsewhere; the coordinates have been deposited in the RCSB Protein Data Bank (PDB ID: 5M96).

gen atoms of the methylpyrimidine group make water-mediated hydrogen bonds to residues R367, L287, and E379, while the adjacent amide NH group makes a hydrogen bond with the carbonyl of the backbone of F377. The imidazopyridine group is located in a buried pocket formed by M365, V376, L400, F401, and S404. The methylpiperazine group makes van der Waals contacts with C320, H323, M365, and F388, and the adjacent C=O group of **10** accepts a hydrogen bond from N $\epsilon$ 2-H479. The terminal cyclopentyl group would clash with W317 if helix 12 is in the agonist position. The inverse agonism of **10** is therefore mediated by a ‘push–pull’ mechanism (‘push’ on W317, ‘pull’ on H479) similar to previous reports.<sup>[12]</sup>

In a second round of analogue design, we focused on potential modifications of the cyclopentylamide, which might be a place for oxidative metabolism as observed for **2**. The corresponding *N*-Boc piperazine analogues showed biochemical potency nearly identical to that of the *N*-cyclopropylamide piperazine (data not shown), but were metabolically less stable. The *tert*-butyloxadiazole system is a very well-known stable bioisostere of the Boc group,<sup>[13]</sup> and the three possible regioisomers **33**, **35**, and **36** were synthesized on the newly identified 6,7,8-substituted imidazo[1,2-*a*]pyridine system. The 1,2,4-oxadia-

zoles **33** and **35** showed higher biochemical and cellular potency than the 1,3,4-oxadiazole analogue **36**. Notably, compound **36** showed the highest microsomal stability. Between the two 1,2,4-oxadiazole isomers, oxadiazole **33** with the *tert*-butyl group at position 5 was more potent than analogue **35** with the *tert*-butyl group at position 3. The two isomers have similar shape but different electronic distribution. The nitrogen atoms in the oxadiazoles are strong hydrogen bond acceptors, whereas the oxygen atoms are much weaker.<sup>[14]</sup> In compound **33** the nitrogen adjacent to the oxygen is believed to overlap with the carbonyl group of **10**, thus better mimicking the key C=O...H479 hydrogen bond interaction. The extra nitrogen *ortho* to the *tert*-butyl group is not needed for affinity (i.e., compare **33** with **37**). Assuming a similar overlay, compound **35** has an oxygen atom, a weaker hydrogen bond acceptor, at the position required to make the hydrogen bond with H479, thus being less potent. The two corresponding analogues **33** and **34**, bearing methyl pyrimidine and methyl pyridine amide, respectively, were shown to be 5 to 6 times more potent biochemically than their respective cyclopentylamides **10** and **12**. Unfortunately, this higher biochemical potency did not translate into improved cellular potency. Despite increased stability in RLM, the compounds were less stable in HLM. From **34**, the corresponding isoxazole **37** again showed higher biochemical potency with respect to **12** and a similar loss in the cellular assays despite increased permeation. Finally, six-membered heterocycles to replace the cyclopentylamide were not tolerated, as illustrated with compound **38**.

To monitor cellular off-target inhibition and/or cytotoxicity induced by the compounds, an assay measuring IL-3-induced proliferation of mouse bone marrow cells was performed as previously described.<sup>[15]</sup> Representatives of this compound series did not show any antiproliferative/cytotoxic effects in the mouse bone marrow assay when tested at a maximal concentration of 10  $\mu$ M.

Compounds **10** and **33** were selected for advanced profiling. Both compounds showed no significant inhibition in a representative panel of 30 targets from different classes (all IC<sub>50</sub> > 10  $\mu$ M) and good selectivity over ROR $\beta$  (IC<sub>50</sub>: > 10 and 2.7  $\mu$ M for **10** and **33**, respectively) and ROR $\alpha$  (IC<sub>50</sub> > 10  $\mu$ M) in biochemical assays. Introduction of the imidazopyridine core led to lower plasma protein binding (PPB). For instance, **10** and **33** showed free fractions in a rat/human PPB assay of 25.6/31.9% and 10.4/13.8%, respectively, compared with 1.9/3.1% for **2** and < 1% for **1**.

The pharmacokinetic profiles of **10** and **33** were then assessed in rat (Table 2). Both compounds showed similar profiles with moderate to low volumes of distribution (*V*<sub>SS</sub>) and short MRT and *t*<sub>max</sub>. Compound **33** showed a lower clearance rate than **10** which may be attributed to the switch from a cyclopentyl to a *tert*-butyl side chain, which is less prone to oxidative metabolism. In addition, **33** showed a greater oral bioavailability. When free drug exposure was taken into account, **10** and **33** showed similar free AUC and *C*<sub>max</sub> values. Both compounds were therefore further tested in a rat PK/PD model.

To generate antigen-specific cells *in vivo*, a delayed-type hypersensitivity (DTH) study was performed. Female Lewis rats

Parameter	<b>10</b>	<b>33</b>
Dose (i.v./p.o.) [mg kg <sup>-1</sup> ]	1.0/3.0	1.0/3.0
CL [mL min <sup>-1</sup> .kg <sup>-1</sup> ]	48 ± 6	26
V <sub>SS</sub> [L.kg <sup>-1</sup> ]	3.0 ± 1.5	2.1
t <sub>1/2</sub> [h]	4.5 ± 2.6	1.3
MRT [h]	1.1 ± 0.7	1.4
AUC i.v. d.n. free [nm h] <sup>[a]</sup>	188 ± 26	132
AUC p.o. d.n. free [nm h] <sup>[a]</sup>	44 ± 11	58 ± 12
F [%]	23 ± 4	44 ± 9
C <sub>max</sub> d.n. free [nM] <sup>[a]</sup>	27 ± 8	23 ± 7
t <sub>max</sub> [h]	0.3 ± 0.0	0.5 ± 0.0
PPB rat/human [%]	74.4/68.8	89.6/86.2

[a] d.n.: dose normalized.

were sensitized with 100 µg methylated bovine serum albumin (BSA) in complete Freund's adjuvant (DIFCO). Fourteen days after sensitization, rats were challenged with 10 µL methylated BSA into the right ear and with 10 µL 5% glucose into the left ear. Compounds **10** and **33** were dosed twice daily by oral gavage starting just before the antigen challenge until the end of the study (50 h, necropsies were carried out 2 h post-final dose). Cells were harvested from the draining popliteal lymph nodes and were used in ex vivo recall assays to assess IL-17A pathway inhibition by the compounds. Cells were seeded into 96-well microtiter plates (4 × 10<sup>5</sup> cells per well) and antigen-specific T cells were re-stimulated with methylated BSA (50 µg mL<sup>-1</sup>) or with the lectin ConA and incubated for 72 h. Supernatants were collected, and IL-17A cytokine concentrations were determined by ELISA (Table 3).

	<b>10</b> <sup>[a]</sup>	<b>33</b> <sup>[a]</sup>
ConA stimulation: inhibition of IL-17A production [%]	-62	-71
mBSA stimulation: inhibition of IL-17A production [%]	-77	-81
Blood-free exposure at 2 h [nm]	481 ± 103	149 ± 20

[a] Tested at 15 mg kg<sup>-1</sup> p.o.

Compounds **10** and **33** were found to be potent inhibitors of IL-17A production by ConA or after methylated BSA stimulation of draining lymph node cells. Notably, free exposure of **10** at 2 h was over-proportional to that expected based on PK data, whereas **33** was in the expected range. Measured free drug exposures are in line with the IC<sub>50</sub> values from the in vitro cellular assays for the observed PD effect with a decrease in IL-17A production.

In conclusion, we have developed a new series of RORγt inverse agonists based on an imidazopyridine core showing good pharmacological potencies, physicochemical profiles, and excellent selectivity as illustrated by compound **10**. In addition, replacement of the cyclopentylamide by a *tert*-butyloxadiazole led to inhibitor **33** with increased rat metabolic stability in vitro

and in vivo. This new imidazopyridine scaffold showed decreased plasma protein binding across species leading to higher free fractions. Compounds **10** and **33** had good oral PK and decreased IL-17A production at low doses in vivo in a PK/PD experiment. We believe that such compounds are excellent tool compounds to further explore the in vivo biology around RORγt inhibition. Indeed, more data from in vivo pharmacology studies using **10** will be published in a separate paper.

## Experimental Section

**General:** Chemicals were purchased from commercial sources and were used without further purification. Reactions were magnetically and mechanically stirred and monitored by thin-layer chromatography (TLC) on Merck silica gel 60F<sub>254</sub> glass plates (visualized by UV fluorescence at λ = 254 nm) or analytical Waters Acquity UPLC instrument equipped with PDA detector, Waters Acquity SQD mass spectrometer and Waters Acquity HSS T3 1.8 µm 2.1 × 50 mm column. Peak detection is reported at full scan 210–450 nm eluting with a gradient composed of water/0.05% formic acid/3.75 mM ammonium formate and acetonitrile/0.05% formic acid. Mass spectrometry results are reported as the ratio of mass over charge. The purity of new compounds was >95%, as determined by <sup>1</sup>H NMR and LC–MS after chromatography. Flash column chromatography was performed with Biotage® SNAP silica gel cartridges, eluting with distilled technical-grade solvents on an Isolera One apparatus from Biotage. NMR data were recorded on a Bruker spectrometer operating at 600 MHz. Chemical shifts (δ) are reported in ppm. The data are reported as: s = singlet, d = doublet, t = triplet, q = quadruplet, m = multiplet, and bs = broad singlet.

**8-Bromo-7-methyl-6-nitroimidazole[1,2-*a*]pyridine **5**:** A mixture of 3-bromo-4-methyl-5-nitropyridin-2-amine **4** (27.4 g, 118 mmol) and 2-chloroacetyl aldehyde (50 wt% in water, 74.2 g, 4 equiv) was stirred at 90 °C for 3 h. The mixture was cooled to RT and diluted with 100 mL of MeOH before the volatiles were removed in vacuo. To the residue, 100 mL of CH<sub>2</sub>Cl<sub>2</sub> were added and the mixture was stirred for few minutes. The resulting precipitate was filtered off, washed with CH<sub>2</sub>Cl<sub>2</sub> and after high vacuum drying, the title compound was obtained as a beige solid (33 g, quant., 93% purity) which was used without further purification. MS (*m/z*): 256.2/258.2 [*M*+H]<sup>+</sup>; <sup>1</sup>H NMR (600 MHz, [D<sub>6</sub>]DMSO): δ = 9.86 (s, 1H), 8.37 (s, 1H), 8.01 (s, 1H), 2.68 ppm (s, 3H).

**8-Bromo-7-methylimidazo[1,2-*a*]pyridin-6-amine **6**:** A mixture of 8-bromo-7-methyl-6-nitroimidazole[1,2-*a*]pyridine **5** (33 g, 129 mmol), iron powder (14.39 g, 2 equiv) and ammonium chloride (36.5 g, 5.3 equiv) in 650 mL of EtOH was held at reflux for 18 h. Additional iron powder was added, and the mixture was held at reflux until the starting material was fully consumed. Upon completion, the mixture was cooled down and the volatiles were removed in vacuo. The crude residue was partitioned between 1 L of CH<sub>2</sub>Cl<sub>2</sub>/MeOH (95:5) and 200 mL of a 5% aqueous NaHCO<sub>3</sub> solution. The organic phase was separated and the aqueous phase was further extracted three times with 300 mL of CH<sub>2</sub>Cl<sub>2</sub>/MeOH (95:5). The organic phases were combined, dried over sodium sulfate and concentrated in vacuo to afford the crude title compound (18.8 g, 43.1%, 69% purity) which was used without further purification. MS (*m/z*): 226.2/228.2 [*M*+H]<sup>+</sup>; <sup>1</sup>H NMR (600 MHz, [D<sub>6</sub>]DMSO): δ = 7.91 (s, 1H), 7.86 (s, 1H), 7.49 (s, 1H), 5.83–4.39 (m, 2H), 2.34 ppm (s, 3H).

***N*-(8-Bromo-7-methylimidazo[1,2-*a*]pyridin-6-yl)-2-methylpyrimidine-5-carboxamide **7**:** To a mixture of 8-bromo-7-methylimida-

zo[1,2-*a*]pyridin-6-amine **6** (8.0 g, 35.4 mmol), 2-methylpyrimidine-5-carboxylic acid (6.11 g, 1.25 equiv) and triethylamine (10.74 g, 3 equiv) in 250 mL CH<sub>2</sub>Cl<sub>2</sub>, propylphosphonic anhydride (T3P; 50 wt % in EtOAc, 33.8 g, 1.5 equiv) was added dropwise. The resulting mixture was stirred at RT for 18 h. To complete the reaction, 2-methylpyrimidine-5-carboxylic acid (3 g), triethylamine (10 mL) and T3P (50 wt % in EtOAc, 15 mL) were added and the mixture was stirred for another 18 h at RT. Saturated NaHCO<sub>3</sub> aqueous solution was added to the reaction mixture. The resulting insoluble material was filtered off, washed with water and after high vacuum drying, 6.9 g of the title compound were obtained as a beige solid. The organic phase was dried over sodium sulfate and the solvents were removed in vacuo, the crude residue was purified by flash chromatography eluting with CH<sub>2</sub>Cl<sub>2</sub>/MeOH (100:0 to 80:20) to afford 1.08 g of the title compound. Compound **7** was obtained as a beige solid with a total recovery of 7.98 g (59% yield). MS (*m/z*): 346.1/348.1 [*M*+H]<sup>+</sup>; <sup>1</sup>H NMR (600 MHz, [D<sub>6</sub>]DMSO): δ = 10.54 (s, 1H), 9.23 (s, 2H), 8.74 (s, 1H), 8.09 (s, 1H), 7.62 (s, 1H), 2.74 (s, 3H), 2.40 ppm (s, 3H).

**Potassium (S)-((4-(*tert*-butoxycarbonyl-3-methylpiperazin-1-yl)-methyl)trifluoroborate **8****: A mixture of potassium (bromomethyl)-trifluoroborate (30 g, 139 mmol) and (S)-1-*N*-Boc-2-methylpiperazine (31.4 g, 1.05 equiv) in 150 mL of THF was held at reflux under nitrogen atmosphere for 18 h. The mixture was cooled to RT and the solvent was removed in vacuo. The residue was taken up in 900 mL of acetone and potassium carbonate (41.3 g, 2 equiv) was added. The resulting mixture was stirred at RT for 18 h. The precipitate was filtered off, washed with acetone and after high vacuum drying, the title compound was obtained as a white powder (42.05 g, 88% yield) and was used without further purification. MS (*m/z*): 280.2/281.2/282.2 [*M*-H]<sup>-</sup>; <sup>1</sup>H NMR (600 MHz, [D<sub>6</sub>]DMSO, 100 °C): δ = 4.14 (m, 1H), 3.72 (m, 1H), 3.17–2.96 (m, 3H), 2.47–2.16 (bm, 2H), 1.65 (bs, 2H), 1.42 (s, 9H), 1.20 (d, 3H).

**(S)-*tert*-Butyl-2-methyl-4-((7-methyl-6-(2-methylpyrimidine-5-carboxamido)imidazo[1,2-*a*]pyridin-8-yl)methyl)piperazine-1-carboxylate **9****: To a degassed solution of *N*-(8-bromo-7-methylimidazo[1,2-*a*]pyridin-6-yl)-2-methylpyrimidine-5-carboxamide **7** (3.63 g, 10.49 mmol), potassium (S)-((4-(*tert*-butoxycarbonyl-3-methylpiperazin-1-yl)methyl)trifluoroborate **8** (6.72 g, 2 equiv), X-Phos (750 mg, 0.15 equiv) and cesium carbonate (10.25 g, 3 equiv) in 60 mL THF/water (9:1), palladium acetate (177 mg, 0.075 equiv) was added and the mixture was then stirred under argon atmosphere at 80 °C for 40 h. The mixture was diluted with EtOAc and washed with saturated NaHCO<sub>3</sub>. The organic phase was separated, dried over sodium sulfate and the resulting crude residue was purified by flash chromatography eluting with CH<sub>2</sub>Cl<sub>2</sub>/MeOH (99:1 to 90:10) to afford the titled compound as a light-yellow solid (3.98 g, 79% yield). MS (*m/z*): 480.4 [*M*+H]<sup>+</sup>; <sup>1</sup>H NMR (600 MHz, [D<sub>6</sub>]DMSO): δ = 10.29 (s, 1H), 9.22 (s, 2H), 8.63 (s, 1H), 7.91 (s, 1H), 7.53 (s, 1H), 4.07 (bs, 1H), 3.91 (m, 2H), 3.64 (m, 1H), 2.86 (m, 1H), 2.73 (s, 3H), 2.62 (m, 2H), 2.36 (s, 3H), 2.20 (m, 1H), 2.00 (m, 1H), 1.39 (s, 9H), 1.08 ppm (2 s, 3H).

**(S)-*N*-(8-((4-(Cyclopentanecarbonyl)-3-methylpiperazin-1-yl)-methyl)-7-methylimidazo[1,2-*a*]pyridin-6-yl)-2-methylpyrimidine-5-carboxamide **10****: 1) (S)-2-methyl-*N*-(7-methyl-8-((3-methylpiperazin-1-yl)methyl)imidazo[1,2-*a*]pyridin-6-yl)pyrimidine-5-carboxamide hydrochloride salt. To a solution of (S)-*tert*-butyl-2-methyl-4-((7-methyl-6-(2-methylpyrimidine-5-carboxamido)imidazo[1,2-*a*]pyridin-8-yl)methyl)piperazine-1-carboxylate **9** (3.97 g, 8.28 mmol) in 70 mL of CH<sub>2</sub>Cl<sub>2</sub>, 4 M HCl in dioxane (20.7 mL, 10 equiv) was added. The resulting mixture was stirred at RT for 2 h. The resulting precipitate was filtered off, washed with *tert*-bu-

tylmethyl ether and after high-vacuum drying, the titled compound was isolated as a white powder (3.91 g, 90% yield) and was used without further purification.

2) **(S)-2-Methyl-*N*-(7-methyl-8-((3-methylpiperazin-1-yl)methyl)imidazo[1,2-*a*]pyridin-6-yl)pyrimidine-5-carboxamide hydrochloride salt** (3.91 g, 7.44 mmol), cyclopentanecarboxylic acid (1.02 g, 1.02 equiv) and triethylamine (7.26 mL, 7 equiv) were dissolved in 100 mL of CH<sub>2</sub>Cl<sub>2</sub> and then, T3P (50 wt % in EtOAc, 5.9 g, 1.2 equiv) was added dropwise. The resulting mixture was stirred at RT for 18 h and then washed with saturated NaHCO<sub>3</sub> aqueous solution twice. The aqueous phases were combined and extracted with CH<sub>2</sub>Cl<sub>2</sub>. The organic phases were combined, washed with brine, dried over sodium sulfate and concentrated in vacuo to afford a light-yellow foam. The crude compound was purified by flash chromatography eluting with CH<sub>2</sub>Cl<sub>2</sub>/MeOH (99:1 to 90:10) to afford the titled compound as an off-white solid (2.6 g, 72.7% yield). MS (*m/z*): 476.4 [*M*+H]<sup>+</sup>; <sup>1</sup>H NMR (600 MHz, [D<sub>6</sub>]DMSO): δ = 10.29 (s, 1H), 9.22 (s, 2H), 8.64 (s, 1H), 7.92 (s, 1H), 7.53 (s, 1H), 4.53 (bs, 0.5H), 4.17 (m, 1H), 4.0–3.85 (m, 2H), 3.71 (d, 0.5H), 3.10 (t, 0.5H), 2.90 (m, 1H), 2.75–2.55 (m, 5.5H), 2.37 (s, 3H), 2.17 (m, 1H), 1.98 (m, 1H), 1.85–1.45 (m, 8H), 1.17 and 1.05 ppm (d, 3H).

**(S)-*N*-(8-((4-(5-(*tert*-Butyl)-1,2,4-oxadiazol-3-yl)-3-methylpiperazin-1-yl)methyl)-7-methylimidazo[1,2-*a*]pyridin-6-yl)-2-methylpyrimidine-5-carboxamide **33****: 1) (S)-*N*-(8-((4-cyano-3-methylpiperazin-1-yl)methyl)-7-methylimidazo[1,2-*a*]pyridin-6-yl)-2-methylpyrimidine-5-carboxamide. At 0 °C, to a solution of (S)-2-methyl-*N*-(7-methyl-8-((3-methylpiperazin-1-yl)methyl)imidazo[1,2-*a*]pyridin-6-yl)pyrimidine-5-carboxamide hydrochloride salt (2.84 g, 5.05 mmol) in 50 mL of CH<sub>2</sub>Cl<sub>2</sub>, DIPEA (3.26 g, 5 equiv) was added followed by BrCN (3 M in CH<sub>2</sub>Cl<sub>2</sub>, 1.68 mL, 1 equiv). The mixture was stirred at RT for 1 h and then quenched by addition of brine. The organic phase was separated, dried over sodium sulfate and concentrated in vacuo to afford the titled compound as a crude beige oil (2.05 g, quant.) which was used without further purification.

2) **(S)-*N*-(8-((4-(*N*-Hydroxycarbamidoyl)-3-methylpiperazin-1-yl)methyl)-7-methylimidazo[1,2-*a*]pyridin-6-yl)-2-methylpyrimidine-5-carboxamide**. A mixture of (S)-*N*-(8-((4-cyano-3-methylpiperazin-1-yl)methyl)-7-methylimidazo[1,2-*a*]pyridin-6-yl)-2-methylpyrimidine-5-carboxamide (2.05 g, 5.05 mmol) and hydroxylamine (50 wt % in water, 1.33 g, 4 equiv) in 50 mL of EtOH was held at reflux for 2 h. The mixture was concentrated to dryness in vacuo to afford a crude brown oil (2.2 g) which was used without further purification in the next step.

3) **(S)-*N*-(8-((4-(5-(*tert*-Butyl)-1,2,4-oxadiazol-3-yl)-3-methylpiperazin-1-yl)methyl)-7-methylimidazo[1,2-*a*]pyridin-6-yl)-2-methylpyrimidine-5-carboxamide **33****. A mixture of the crude (S)-*N*-(8-((4-(*N*-hydroxycarbamidoyl)-3-methylpiperazin-1-yl)methyl)-7-methylimidazo[1,2-*a*]pyridin-6-yl)-2-methylpyrimidine-5-carboxamide (2.2 g, 5.05 mmol), pivalic anhydride (3.76 g, 4 equiv) and trimethylamine (3.26 g, 5 equiv) in 100 mL of CH<sub>2</sub>Cl<sub>2</sub> was stirred at RT for 2 h and then held at reflux for 16 h. The mixture was washed with saturated aqueous NaHCO<sub>3</sub> solution twice. The aqueous phases were combined and extracted with CH<sub>2</sub>Cl<sub>2</sub>. The organic phases were combined, washed with brine, dried over sodium sulfate and concentrated in vacuo to afford the crude compound which was purified by flash chromatography eluting with CH<sub>2</sub>Cl<sub>2</sub>/MeOH (99:1 to 90:10) to afford the title compound as an off-white solid (1.04 g, 40.9% yield). MS (*m/z*): 504.4 [*M*+H]<sup>+</sup>; <sup>1</sup>H NMR (600 MHz, [D<sub>6</sub>]DMSO): δ = 10.26 (s, 1H), 9.20 (s, 2H), 8.63 (s, 1H), 7.91 (s, 1H), 7.52 (s, 1H), 3.94 (q, 3H), 3.48 (d, 1H), 3.15 (d, 1H), 3.10–2.96 (m,

1H), 2.71 (s, 4H), 2.64 (d, 1H), 2.37 (s, 3H), 2.19 (dt, 1H), 1.30 (s, 9H), 1.11 ppm (d, 3H).

**TR-FRET assay:** The activity of test compounds to displace a RIP140 co-activator derived biotinylated peptide from the ROR $\gamma$  ligand binding domain was measured. The assay mixture (16  $\mu$ L) included 5 nM recombinant His<sub>6</sub>-tagged human ROR $\gamma$  ligand binding domain comprising amino acids 264–518, 90 nM biotinylated RIP140 co-activator peptide (Biotin-NH-Ahx-NSH QKV TLL QLL LGH KNE EN-CONH<sub>2</sub>, 0.45 nM Cy5-labelled streptavidin, and 1.5 nM europium-labeled anti-His<sub>6</sub> antibody. After incubation of assay plates for 1 h at room temperature, donor (615 nm) and acceptor (665 nm) emission values were recorded using an EnVision 2102 multilabel reader. Concentration–response curves for IC<sub>50</sub> determinations were constructed from the 665/615 nm emission ratio using the GraphPad Prism software package.

**Gal4-ROR $\gamma$ -hinge-LBD luciferase reporter gene assay.** A Jurkat cell line stably expressing a pGL4.35 reporter plasmid (Promega) was generated; this plasmid contains nine repeats of the Gal4 upstream activator sequence driving the transcription of the luciferase gene. A vector containing the human ROR $\gamma$ -hinge-LBD fused to the DNA-binding domain (DBD) of the Gal4 gene (Promega) was cloned. Jurkat cells containing the reporter plasmid were transfected with the ROR $\gamma$ -hinge-LBD fusion plasmid and clones stably expressing the two constructs were generated. Cells were resuspended in RPMI 1640 medium containing supplements and 100 U mL<sup>-1</sup> penicillin and 100 mg mL<sup>-1</sup> streptomycin, and were seeded in microtiter plates (5  $\times$  10<sup>4</sup> cells per well). The ROR $\gamma$  inhibitors or DMSO as a control were added to the cells, after 24 h of incubation, cells were lysed (Steady lite plus, PerkinElmer) and luciferase activity was measured using an EnVision Multilabel Plate Reader (PerkinElmer).

**Human Th17 cell assays.** Peripheral blood mononuclear cells were isolated from human buffy coats by density gradient centrifugation using Ficoll-Paque. CD4<sup>+</sup> T cells were obtained by immunomagnetic isolation using a CD4<sup>+</sup> T-Cell Enrichment Kit according to the manufacturer's instructions (Stem Cell). CD4<sup>+</sup> T cells were seeded at 5  $\times$  10<sup>4</sup> cells per well in CD3 and CD28 pre-coated microtiter plates and were cultured with a cytokine cocktail containing IL-6 (20 ng mL<sup>-1</sup>), TGF- $\beta$ 1 (5 ng mL<sup>-1</sup>), IL-1 $\beta$  (10 ng mL<sup>-1</sup>), and IL-23 (10 ng mL<sup>-1</sup>). Compounds were added at the beginning of the cell cultures, and supernatants were collected after 72 h of incubation. Supernatants were collected, and IL-17A cytokine concentration was quantified by ELISA.

**Human whole-blood assay.** Heparinized whole blood was obtained from healthy volunteers and was diluted with high-glucose DMEM containing supplements, 100 U mL<sup>-1</sup> penicillin, and 100 mg mL<sup>-1</sup> streptomycin. Diluted blood (20% final concentration) was incubated with compounds and was stimulated with 10  $\mu$ g mL<sup>-1</sup> ConA and 10 ng mL<sup>-1</sup> recombinant human IL-23. After 72 h incubation supernatants were collected for IL-17A cytokine quantification by ELISA according to the manufacturer's instructions (Bender Medsystems).

**Approval for the use of humans and animals in research:** Blood from healthy volunteers was provided under informed consent and collected through the Novartis Tissue Donor Program (TRIO128) in accordance with the Swiss Human Research Act and approval of the responsible ethic committee (Ethikkommission Nordwest- und Zentralschweiz number: 329/13). Buffy coats from healthy volunteers were provided under informed consent and collected through the InterRegionale Blutspende of the Swiss Red Cross. The rat experiments were performed in accordance with the animal ex-

perimentation guidelines and laws laid down by the Swiss Federal and Cantonal Authorities, and specifically as described in Basel-Stadt Experimental License No. 1244.

## Acknowledgements

We thank Engin Tasdelen, Alex Bussenault, Ralf Boesch, Richard Felber, Celine Dubois, Florence Ecoeur, Jessica Weiss, Julia Riker, Bernhard Jost, Yves Henriquez, Elodie Arduin, Aude Izaac, Celine Be, and Elke Koch for their excellent assistance.

**Keywords:** imidazopyridines · inverse agonists · oxadiazoles · plasma protein binding · ROR $\gamma$

- [1] A. M. Jetten, *Nucl. Recept. Signaling* **2009**, *7*, 1–32.
- [2] a) S. Xiao, N. Yosef, J. Yang, Y. Wang, L. Zhou, C. Zhu, C. Wu, E. Baloglu, D. Schmidt, R. Ramesh, M. Lobera, M. S. Sundrud, P.-Y. Tsai, Z. Xiang, J. Wang, Y. Xu, X. Lin, K. Kretschmer, P. B. Rahl, R. A. Young, Z. Zhong, D. A. Hafler, A. Regev, S. Ghosh, A. Marson, V. K. Kuchroo, *Immunity* **2014**, *40*, 477–479; b) J. Skepner, R. Ramesh, M. Trocha, D. Schmidt, E. Baloglu, M. Lobera, T. Carlson, J. Hill, L. A. Orband-Miller, A. Barnes, M. Boudjelal, M. Sundrud, S. Ghosh, J. Yang, *J. Immunol.* **2014**, *192*, 2564–2575; c) M. R. Chang, B. Lyda, T. M. Kamenecka, P. R. Griffin, *Arthritis Rheumatol.* **2014**, *66*, 579–588.
- [3] D. J. Kojetin, T. P. Burris, *Nat. Rev. Drug Discovery* **2014**, *13*, 197–216.
- [4] P. Cyr, S. M. Bronner, J. J. Crawford, *Bioorg. Med. Chem. Lett.* **2016**, *26*, 4387–4393.
- [5] C. Gege, *Expert Opin. Ther. Pat.* **2016**, *26*, 737–744.
- [6] a) Y. Wang, W. Cai, G. Zhang, T. Yang, Q. Liu, Y. Chen, L. Zhou, Y. Ma, Z. Cheng, S. Lu, Y. G. Zhao, W. Zhang, Z. Xiang, S. Wang, L. Yang, Q. Wu, L. A. Orband-Miller, Y. Xu, J. Zhang, R. Gao, M. Huxdorf, J. X. Xiang, Z. Zhong, J. D. Elliott, X. Lin, *Bioorg. Med. Chem. Lett.* **2014**, *22*, 692–702; b) Y. Wang, W. Cai, Y. Cheng, T. Yang, Q. Liu, G. Zhang, Q. Meng, F. Han, Y. Huang, L. Zhou, Z. Xiang, Y. G. Zhao, Y. Xu, Z. Cheng, S. Lu, Q. Wu, J. N. Xiang, J. D. Elliott, S. Leung, F. Ren, X. Lin, *ACS Med. Chem. Lett.* **2015**, *6*, 787–792.
- [7] a) F. Han, H. Lei, X. Lin, Q. Meng, Y. Wang (Glaxo Group Ltd.), WO2014086894 A1, **2014**; b) J. Deng, H. Lei, X. Ma, X. Lin (GlaxoSmithKline), WO2015180612 A1, **2015**; c) J. Deng, H. Lei, X. Ma, F. Ren, W. Cai, X. Lin (GlaxoSmithKline), WO2015180613 A1, **2015**; d) H. Lei, X. Ma, F. Ren, X. Lin, R. W. Marquis, Jr. (Glaxo Group Ltd.), WO2015180614 A1, **2015**.
- [8] a) J. R. Blinn, A. C. Flick, G. M. Wennerstal, P. Jones, N. Kaila, J. R. Kiefer, Jr., R. G. Kurumbail, S. R. Mente, M. J. Meyers, M. E. Schnute, A. Thorensen, L. Xing, E. Zamaratski, C. W. Zapf (Pfizer Inc.), WO2015015378 A3, **2015**; b) A. C. Flick, P. Jones, N. Kaila, S. R. Mente, M. E. Schnute, J. D. Truzpek, M. L. Vazquez, L. Xing, L. Zhang, G. M. Wennerstal, E. Zamaratski (Pfizer Inc.), WO2016046755 A1, **2016**.
- [9] M. H. Norman, K. L. Andrews, Y. Y. Bo, S. K. Booker, S. Caenepeel, V. J. Cee, N. D. D'Angelo, D. J. Freeman, B. J. Herberich, F. T. Hong, C. L. M. Jackson, J. Jiang, B. A. Lanman, L. Liu, J. D. McCarter, E. L. Mullady, N. Nishimura, L. H. Pettus, A. B. Reed, T. S. Miquel, A. L. Smith, M. M. Stec, S. Tadesse, A. Tasker, D. Aidasani, X. Zhu, R. Subramanian, N. A. Tamayo, L. Wang, D. A. Whittington, B. Wu, T. Wu, R. P. Wurtz, K. Yang, L. Zalameda, N. Zhang, P. E. Hughes, *J. Med. Chem.* **2012**, *55*, 7796–7816.
- [10] J. Yin, B. Xiang, M. A. Huffman, C. E. Raab, I. W. Davies, *J. Org. Chem.* **2007**, *72*, 4554–4557.
- [11] a) For 1,2,4-oxadiazole: J. S. Scott, A. M. Birch, K. J. Brocklehurst, A. Broo, H. S. Brown, R. J. Butlin, D. S. Clarke, O. Davidsson, A. Ertan, K. Goldberg, S. D. Groombridge, J. A. Hudson, D. Laber, A. G. Leach, P. A. MacFaul, D. McKerrecher, A. Pickup, P. Schofield, P. H. Svensson, P. Sorme, J. Teague, *J. Med. Chem.* **2012**, *55*, 5361–579; b) For 1,3,4-oxadiazole: A. Ashworth, C. J. Lord, R. J. R. Elliott, D. Niculescu-Duvaz, R. A. Porter, R. Aqil, R. J. Boffey, M. J. Bayford, S. Firth-Clark, A. Hopkins, A. N. Jarvis, T. R. Perrior, P. A. Skone, R. E. Key, (Royal Cancer Hospital, Institute of Cancer Research, UK), WO2015036759, **2015**.

- [12] a) R. I. Olsson, Y. Xue, S. von Berg, A. Aagaard, J. McPheat, E. L. Hansson, J. Bernström, P. Hansson, J. Jirholt, H. Grindebacke, A. Leffler, R. Chen, Y. Xiong, H. Ge, T. G. Hansson, F. Narjes, *ChemMedChem* **2016**, *11*, 207–216; b) O. René, B. P. Fauber, G. de Leon Boenig, B. Burton, C. Eiden-schenk, C. Everett, A. Gobbi, S. G. Hymowitz, A. R. Johnson, J. R. Kiefer, M. Liimatta, P. Lockey, M. Norman, W. Ouyang, H. A. Wallweber, H. Wong, *ACS Med. Chem. Lett.* **2015**, *6*, 276–281.
- [13] J. S. Scott, A. M. Birch, K. J. Brocklehurst, A. Broo, H. S. Brown, K. Goldberg, S. D. Groombridge, J. A. Hudson, A. G. Leach, P. A. MacFaul, D. McKerrecher, R. Poultney, P. Schofield, P. H. Svensson, *MedChemComm* **2013**, *4*, 95–100.
- [14] P. W. Kenny, C. A. Montanari, I. M. Prokopczyk, J. F. R. Ribeiro, G. R. Sartori, *J. Med. Chem.* **2016**, *59*, 4278–4288.
- [15] G. Thoma, A. B. Smith, M. J. van Eis, E. Vangrevelinghe, J. Blanz, R. Aichholz, A. Littlewood-Evans, C. C. Lee, H. Liu, H. G. Zerwes, *J. Med. Chem.* **2015**, *58*, 1950–1963.

---

Manuscript received: October 3, 2016

Revised: November 9, 2016

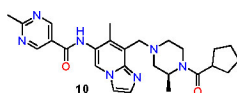
Final Article published: ■ ■ ■ ■, 0000

# COMMUNICATIONS

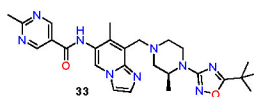
S. Hintermann, C. Guntermann, H. Mattes,  
D. A. Carcache, J. Wagner, A. Vulpetti,  
A. Billich, J. Dawson, K. Kaupmann,  
J. Kallen, R. Stringer, D. Orain\*



## Synthesis and Biological Evaluation of New Triazolo- and Imidazopyridine ROR $\gamma$ t Inverse Agonists



ROR $\gamma$ t FRET IC<sub>50</sub> = 13 nM  
hu-WB Th17 IC<sub>50</sub> = 168 nM  
RLM CL<sub>int</sub> = 30  $\mu$ L min<sup>-1</sup> mg<sup>-1</sup>  
Rat free fraction = 25.6%  
HLM CL<sub>int</sub> = 30  $\mu$ L min<sup>-1</sup> mg<sup>-1</sup>  
human free fraction = 31.9%



ROR $\gamma$ t FRET IC<sub>50</sub> = 2.3 nM  
hu-WB Th17 IC<sub>50</sub> = 282 nM  
RLM CL<sub>int</sub> < 25  $\mu$ L min<sup>-1</sup> mg<sup>-1</sup>  
Rat free fraction = 10.4%  
HLM CL<sub>int</sub> = 96  $\mu$ L min<sup>-1</sup> mg<sup>-1</sup>  
human free fraction = 13.8%

**Autoimmune challenge:** A new series of ROR $\gamma$ t inverse agonists containing triazolo- and imidazopyridine cores has been identified. Compounds based on the 6,7,8-substituted imidazo[1,2-a]pyridine core retained high potencies on the target plus an advantageous physicochemical profile including medium to high free fraction across species. Derivatives **10** and **33** showed in vivo efficacy in a rat PK/PD model and inhibited IL-17A production in an ex vivo challenge.